

Article

Comparison of Quantitative X-ray Diffraction Mineral Analysis Methods

Jingyun Xiao ^{1,2}, Yougui Song ^{1,*}  and Yue Li ¹

¹ State Key Laboratory of Loess and Quaternary Geology, Institute of Earth Environment, Chinese Academy of Sciences, Xi'an 710061, China; xiaojingyun@ieecas.cn (J.X.)

² University of Chinese Academy of Sciences, Beijing 100049, China

* Correspondence: syg@ieecas.cn; Tel.: +86-29-6233-6216

Abstract: X-ray diffraction (XRD) analysis, as one of the most powerful methods, has been widely used to identify and quantify minerals in earth science. How to improve the precision of mineral quantitative analysis is still a hot topic. To date, several quantitative methods have been proposed for different purposes and accompanied by diverse software. In this study, three quantitative mineral analysis methods, including the reference intensity ratio (RIR), Rietveld, and full pattern summation (FPS) methods, are compared and evaluated to systematically investigate their accuracy and applicability. The results show that the analytical accuracy of these methods is basically consistent for mixtures free from clay minerals. However, there are significant differences in accuracy for clay-mineral-containing samples. In comparison, it seems that the FPS method has wide applicability, which is more appropriate for sediments. The Rietveld method has been shown to be capable of quantifying complicated non-clay samples with a high analytical accuracy; nevertheless, most conventional Rietveld software fails to accurately quantify phases with a disordered or unknown structure. The RIR method represents a handy approach but with lower analytical accuracy. Overall, the present results are expected to provide a potentially important reference for the quantitative analysis of minerals in sediments.

Keywords: limit of detection; Rietveld; reference intensity ratio; full pattern summation methods



Citation: Xiao, J.; Song, Y.; Li, Y. Comparison of Quantitative X-ray Diffraction Mineral Analysis Methods. *Minerals* **2023**, *13*, 566. <https://doi.org/10.3390/min13040566>

Academic Editors: Roberto Buccione and Rabah Kechiched

Received: 10 March 2023

Revised: 11 April 2023

Accepted: 12 April 2023

Published: 18 April 2023



Copyright: © 2023 by the authors. Licensee MDPI, Basel, Switzerland. This article is an open access article distributed under the terms and conditions of the Creative Commons Attribution (CC BY) license (<https://creativecommons.org/licenses/by/4.0/>).

1. Introduction

X-ray diffraction (XRD), as an important mineral analysis technique, has been widely employed in geologic research [1–6]. Meanwhile, quantitative analysis of minerals, especially for clay minerals, represents a very promising approach to obtain information on the provenance and weathering intensity of sediment [7–13] and climate change [14–16]. However, it is still a real challenge to accurately quantify mineral composition. The most extensive efforts by far have gone into the mineral quantitative methods, which include the traditional internal standard method [17], external standard method [18], full pattern summation (FPS) [19–22], the reference intensity ratio (RIR) method [23–25], and the increasingly improved Rietveld method [26,27]. However, conventional methods are time-consuming because either pure materials or additional standard materials are artificially added during these test procedures, therefore hampering extensive application. By contrast, the FPS, the RIR, and the Rietveld methods have made considerable progress and been widely used in the last decades, partly due to rapid developments in computer hardware and software [28–31]. The FPS method is based on the principal that the observed diffraction pattern is the sum of signals from the individual phases that compose a sample [19,20,22,32]. The Rietveld method, which differs from single reflection techniques, is a process of refinement between observed and calculated patterns by partial least squares regression based on a crystal structure database [33,34]. The weight of each phase in a sample is obtained from the optimal value of the scale factor during refinement. The RIR

method is also known as the ‘matrix flushing’ method, which depends on the intensity of an individual peak as a reflection of the mineral content by means of the RIR values [23–25].

The accurate quantitative analysis of minerals by XRD is based on the reliable identification of each phase [31]. Therefore, the limit of detection (LOD) of each mineral phase needs to be assessed to show the sensitivity of XRD analysis [35]. Simultaneously, although various software for quantitative mineral analysis have been developed to easily access each method, the knowledge gap about the accuracy of these methods has not yet been filled, impeding our better understanding of their applicability. In particular, the reliability of each method and their source of error remain to be determined, which has left researchers in a dilemma during quantitative analysis. This is largely due to the lack of a systematic contrastive research. As a result, this study aims to address these issues by using artificially mixed samples to test the LOD for the XRD analysis and compare the accuracy and applicability of the three methods. Our results are expected to provide an important reference for the quantitative analysis of minerals in geologic research.

2. Materials and Methods

2.1. Preparation of Artificial Mixture Samples

The amorphous phases (e.g., soil organic matter, etc.), usually ignored as background noise, exert a significant influence on the quantitative accuracy of XRD, even for materials with less amorphous materials [36,37]. Consequently, a high purity of the crystalline phase in the sample should be ensured during quantitative analysis. In this study, seven high-purity minerals including quartz, albite, calcite, dolomite, halite, montmorillonite, and kaolinite were used to prepare the artificial mixture samples, which can approximately represent mineral assemblages in natural sediments. The structural parameters of the above minerals are listed in Table 1. Their purity meets the experimental requirements, as shown by the consistencies of diffraction patterns with corresponding standard references (Figure 1). All the mixture samples were ground into powders of <45 μm (325 mesh), which is suitable for XRD quantitative analysis. Fine grain size is essential to minimize micro-absorption corrections, to give reproducible peak intensities, and to minimize preferred orientation.

Table 1. The crystal structure parameters of selected minerals.

Phase	Quartz	Albite	Calcite	Dolomite	Halite	Kaolinite	Montmorillonite	
Purity	98.83%	99.26%	99.87%	99.88%	98.91%	98.22%	100%	
JADE-PDF#	97-004-1414	00-009-0466	04-008-0788	04-008-0789	97-002-8948	04-010-4800	00-058-2007	
HighScore-COD#	96-900-9667	96-900-1632	96-901-6707	96-900-3509	96-900-3309	96-900-9231	96-900-2780	
TOPAS-COD#	96-210-0188	96-900-1630	96-901-6706	96-900-0573	96-900-3308	96-101-1045	96-900-2779	
JADE-RIR	4.24	2.1	3.24	2.53	5.21	0.98	19.66	
Crystal Structure	Hexagonal	Anorthic	Hexagonal	Hexagonal	Cubic	Monoclinic	Anorthic	
Space Group	P3221 (154)	C-1 (2)	R-3c (167)	R-3 (148)	Fm-3m (225)	C1 (1)	P1 (1)	
Lattice Volume	112.9	332.42	368.07	320.22	179.4	164.95	697.75	
Lattice Parameters	a(Å)	4.912	8.144	4.991	4.8064	5.64	5.1554	5.18
	b(Å)	4.912	12.787	4.991	4.8064	5.64	8.9448	8.98
	c(Å)	5.404	7.16	17.062	16.006	5.64	7.4048	15
	Z	3	2	6	3	4	1	2

Although the minerals used here are standard crystalline phases with high purity, which quantified and verified by HighScore software (version 3.0) (Table 1), the determination of the LOD value is compulsory for each mineral prior to the quantitative experiment. This is because the sensitivity of instrument reflected by the LOD value also potentially determines the accuracy of quantitative analysis result. Thirty-eight samples, each of which was a two-phase mixture of 1 g, were measured for the LOD analyses. In the LOD sample, one phase was the mineral listed in Table 2, and the other was quartz or

corundum as matrix. The phases were weighed by Mettler XS205 DU electronic balance with an accuracy of 1D/100,000, and subsequently mixed and homogenized by hand for 30 min in an agate mortar. All samples were equally divided into three subsamples and then were uniformly filled into the holder for XRD measurements. It was confirmed that each sample was homogenized if the XRD patterns of its three subsamples did not show significant differences.

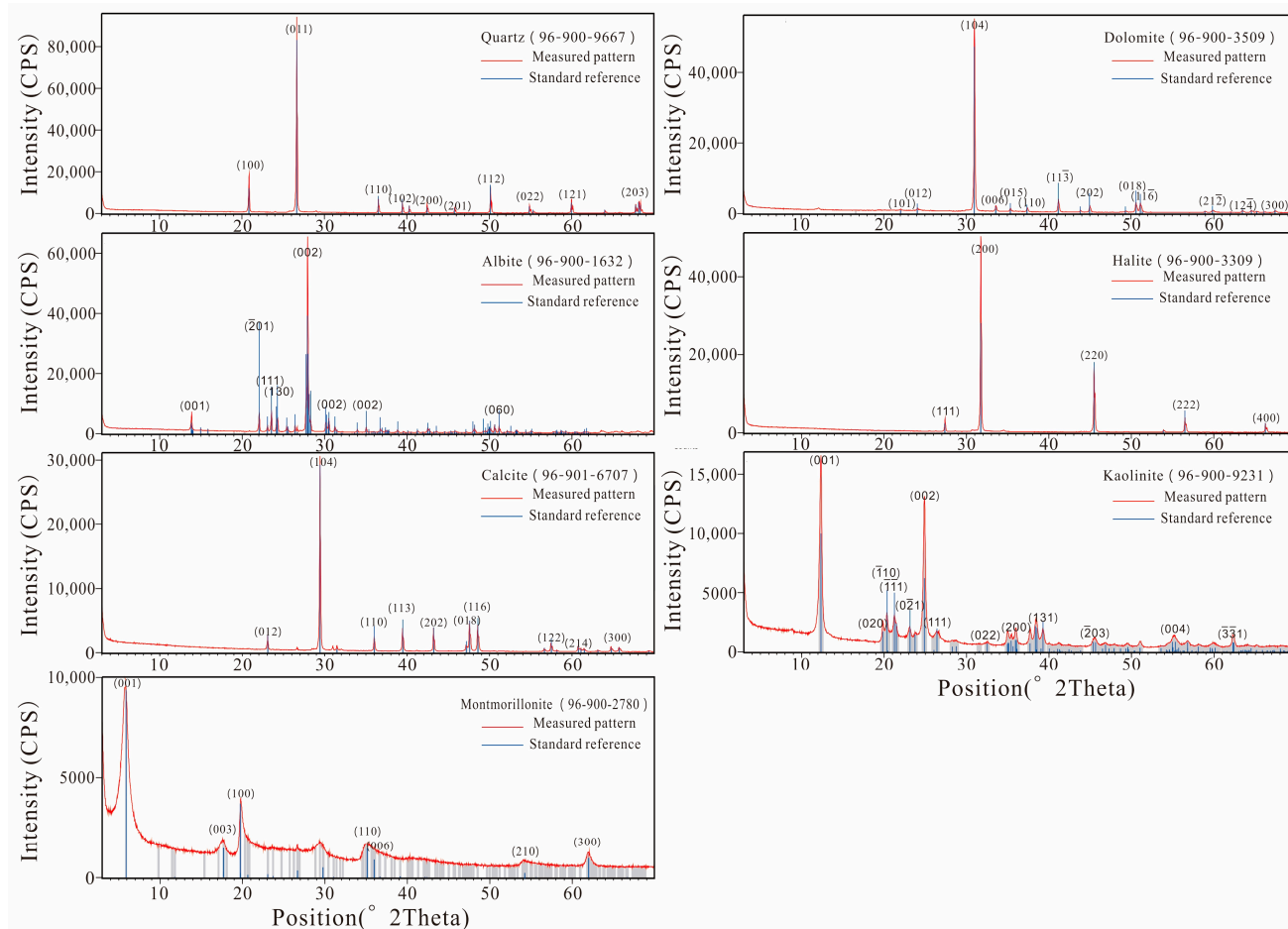


Figure 1. Comparison of X-ray diffraction patterns between 7 kinds of selected minerals and their respective matched standard reference. CPS- counts per second.

Table 2. The limits of detection (LOD) for minerals used in this study. LOD_{cal} is calculated LOD value; LOD_{mea} is measured LOD value in the experiment; LOD_{ref} refers to LOD value from Hillier’s experiment [35].

	Quartz	Calcite	Albite	Dolomite	Kaolinite	Halite	Corundum
RIR	4.04	2.73	2.07	1.94	0.53	5.21	1
(1) LOD _{cal}	0.06%	0.09%	0.12%	0.13%	0.47%	0.05%	/
(2) LOD _{mea}	0.07%	0.06%	0.14%	0.10%	0.80%	0.08%	0.25%
(3) LOD _{ref}	0.17%	0.22%	0.40%	0.25%	0.93%	/	0.43%

The artificial mixtures for quantitative analysis were mixed with different proportions generated randomly in R environment (Appendix A). Six groups of mixtures consisting of 132 samples in total (including 32 samples without clay minerals and 100 samples containing clay mineral phases) were measured for comparative experiments. Each mixture sample had a weight of ~1 g, and the sample preparation method was the same as above.

2.2. Test Conditions

The samples were measured using a Panalytical X'pert Pro X-ray powder diffractometer (Cu K α radiation, $\lambda = 1.5418 \text{ \AA}$) by continuous scanning at the State Key Laboratory of Loess and Quaternary Geology, Institute of Earth Environment, Chinese Academy of Sciences. The diffractometer is equipped with divergence and scattering slits of 1° , anti-scatter slit of 6.6 mm, and the sola slit of 0.04 rad. The sample was scanned from 3° to 70° for the quantitative experiments and from 5° to 40° for the LOD experiments using 40 mA, 40 kV generator settings with a step size of 0.016711° , and a scan speed of $2^\circ/\text{min}$, under constant temperature ($25 \pm 3^\circ\text{C}$) and humidity conditions (60%).

2.3. Quantitative Analysis Applications

The quantitative analysis programs of each method used in this study include: (1) the FPS method, which is automated full pattern summation based on reference library of pure diffraction patterns ('standards'/'reference patterns'), such as FULLPAT [20] and ROCKJOCK [21]; (2) the Rietveld method, which is fitting of the experiment pattern by continuously modifying many parameters based on calibrated crystal structure model, such as HighScore (PANalyticalTM Company, Almelo, The Netherlands) [38], TOPAS (Total Pattern Solution, BrukerTM Company, Karlsruhe, Germany) [39], GSAS (General Structure Analysis System) [40], BGMN [41,42] and Maud [43]; (3) the RIR method, which is carried out by the intensity of the strongest single diffraction peak of each phase with the RIR value, such as an 'easy quantitative' function on JADE.

In following discussions, the HighScore plus software (version 3.0), JADE software (version 9.0), TOPAS software (version 6.0), and ROCKJOCK were used to evaluate performance of each quantitative analysis method. The initial structural models for Rietveld refinement were taken from the International Centre for Diffraction Data (ICDD), Inorganic Crystal Structural Database (ICSD), and Crystallography Open Database (COD). The following parameters were refined: scale factors for all phases, zero-shift parameter, background polynomial coefficients, unit cell parameters for each phase, half-width parameters, atomic site occupancies, atomic coordinates, and preferred orientation. The Rietveld refinement strategy has been described in Madsen and Hill [44] and Young et al. [45] in detail and did not remove background from XRD patterns. The quality of the fit between the calculated and observed diffraction profiles obtained in a Rietveld refinement is usually assessed with the standard agreement Indices R_p , R_{wp} , and R_{exp} , and the goodness of fit index (GOF), defined by Young et al. [46].

2.4. Accuracy Evaluation Model

The cross-validation of results from chemical analysis or other supplemental techniques are always untestable, ascribed to their own systematic error; hence, the known proportion of the artificial mixtures is used as real percentages in this research. The proportion of each phase estimated by different analysis software was the average of three calculations. Subsequently, the absolute error (Δ_{AE}), the relative error (Δ_{RE}), and root mean square error (RMSE) were calculated to indicate the accuracy of these quantitative analysis methods. Although the Δ_{AE} within 3% was generally defined as "highly accurate" in previous studies [47], the error tended to be proportional to the weight of minerals [48]. Thus, the $\pm 3 \text{ wt\%}$ may not be a good representation of accuracy. The equation $y = cX^b$ (where X = concentration in weight, and c and b are constants), relates accuracy with concentration for chemical analysis methods [49]. It has been suggested [35,50] that the uncertainty of a reliable quantitative XRD method should be less than $\pm 50X^{-0.5}$ at the 95% confidence level, which covers all the errors during the analysis, such as weighting errors, counting statistics, instrument errors, etc. Therefore, the model of $y = \pm 50X^{-0.5}$ was introduced to verify the accuracy of results obtained by different quantitative XRD methods visually. Meanwhile, the value of RMSE was also applied to evaluate the error level of each method.

3. Results

3.1. LOD

The LOD values (Table 2) were obtained by extrapolation of the linear regression model established between the weight and the area of characteristic peak for each mineral (Figure 2), where the LOD_s (limit of detection for standard material, which typically is corundum) value was 0.25%. The theoretical LOD values of the other phases were calculated based on the known RIR values and the measured LOD_s according to equation: $\text{LOD} = \text{LOD}_s / \text{RIR}$ [24,35]. The LOD value calculated by the formula is roughly equivalent to that obtained by the linear regression model, which can be verified by each other. It is interesting that these results of the LOD experiment are generally lower than those in Hillier's [35] (Table 2). Thus, it shows that our instrument has high sensitivity to mineral quantitative analysis.

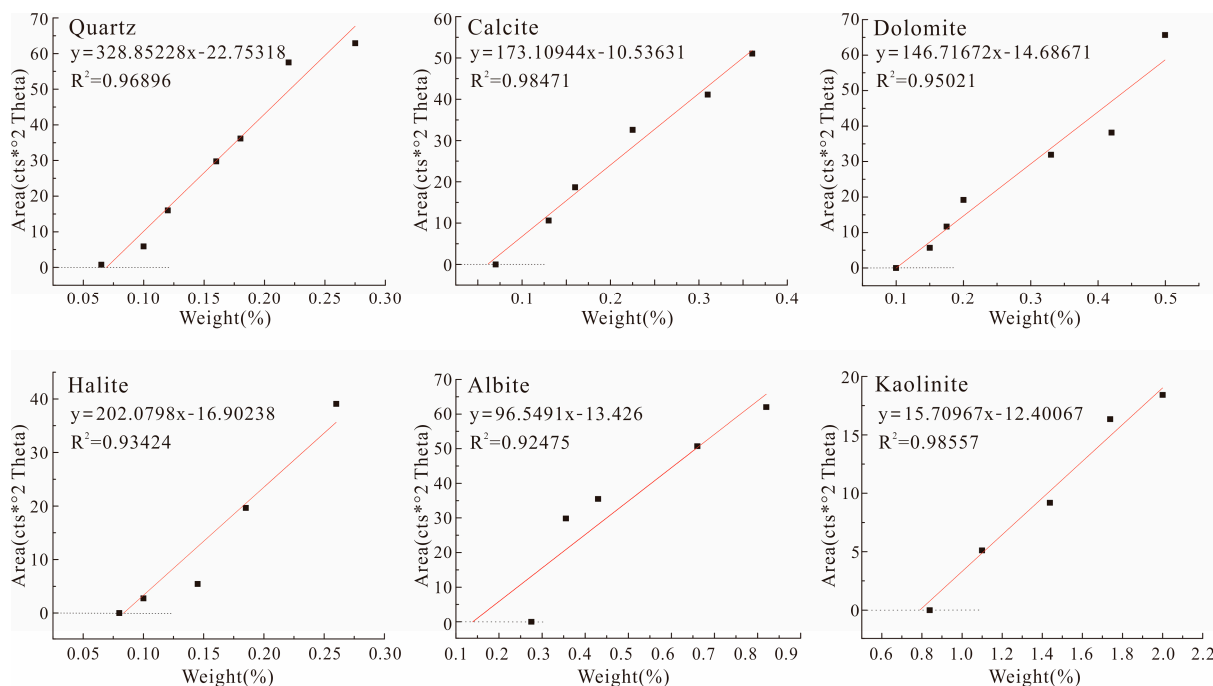


Figure 2. Regression analysis of the content of each mineral and the characteristic peak area. The net integral area of peak is calculated by HighScore during fitting, cts = cps* counting time.

3.2. Accuracy

All samples were tested and qualitatively analyzed under the same conditions (representative samples are shown in Figure 3), but quantitative analysis was conducted with different software. We compared the measured results with the known proportions for each mineral phase in the artificial mixture samples (the raw experiment datasets are listed in the Supplementary Materials Table S1). As shown in Figure 4, the 1:1 line gives an indication of high accuracy for our results. The Δ_{AE} values and the Δ_{RE} values are displayed in Figures 5 and 6, respectively. For the Rietveld method, the earlier findings showed that statistical parameters such as the R_{wp} factor within 15% are necessary for satisfactory quantitative results [51–54]. Thus, we tried to ensure the R_{wp} values were less than 15% during the Rietveld analyses.

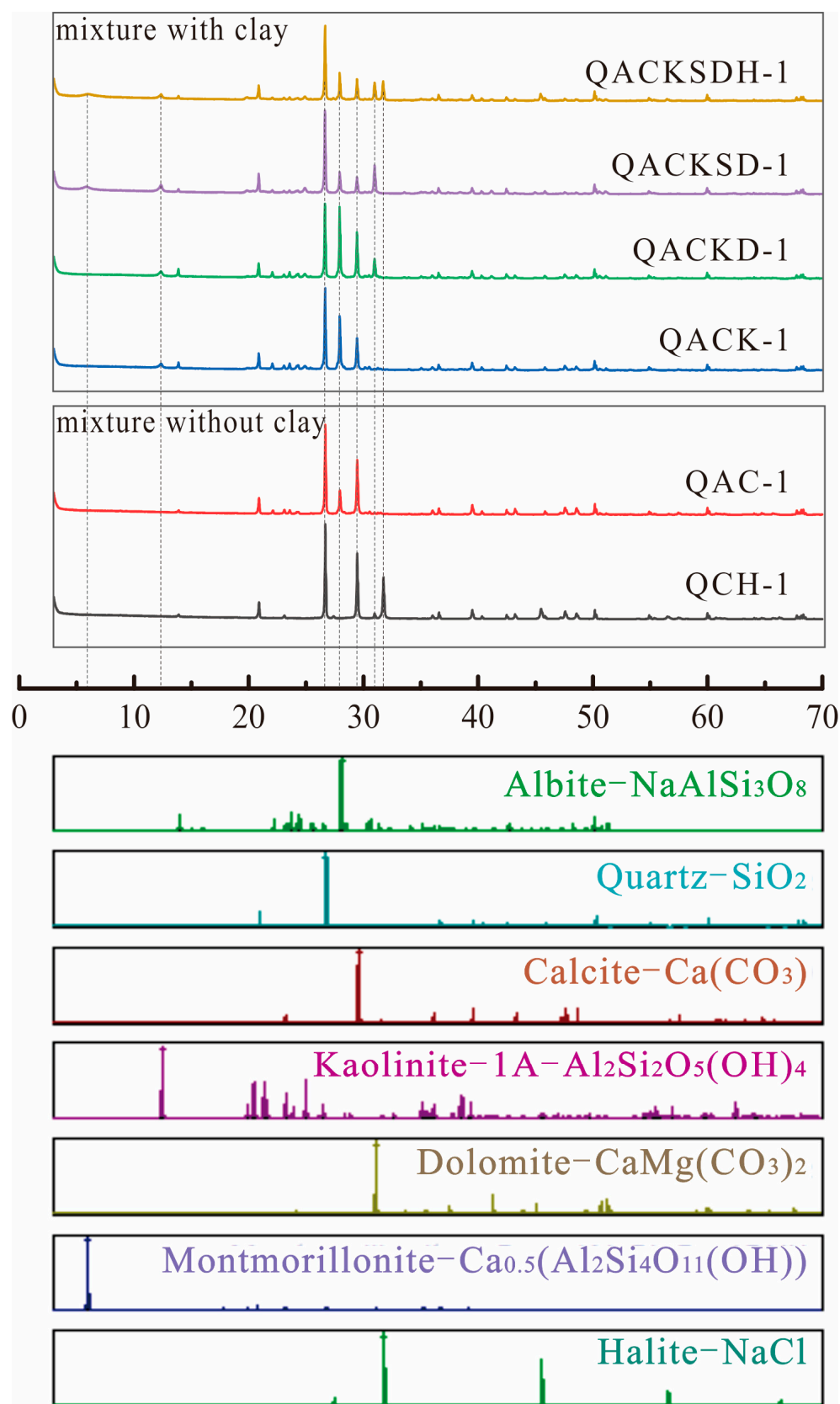


Figure 3. The representative XRD patterns of the mixture samples.

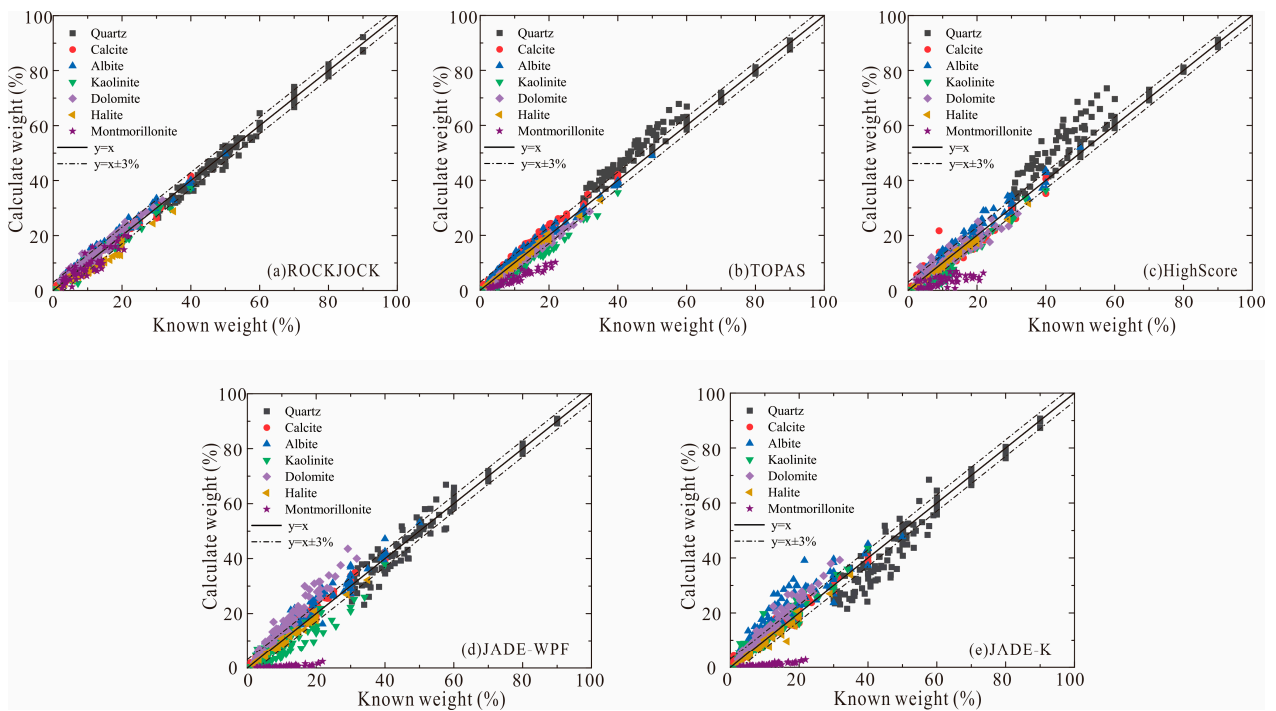


Figure 4. Comparisons of the known and calculated concentrations obtained by different methods. (a) for FPS method by ROCKJOCK; (b) for Rietveld method by TOPAS; (c) for Rietveld method by HighScore; (d) for Whole Pattern Fitting(WPF) and Rietveld Refinement by JADE; (e) for RIR method by JADE.

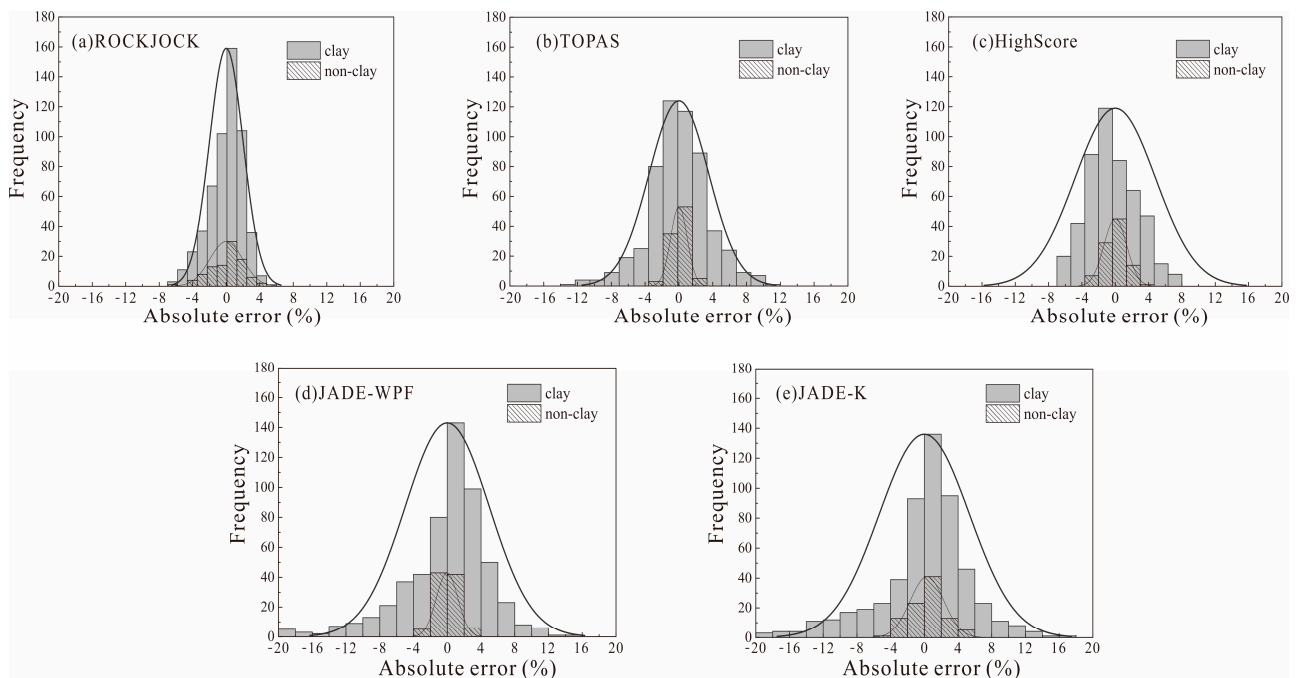


Figure 5. Absolute error frequency distribution of samples. (a) for FPS method by ROCKJOCK; (b) for Rietveld method by TOPAS; (c) for Rietveld method by HighScore; (d) for Whole Pattern Fitting(WPF) and Rietveld Refinement by JADE; (e) for RIR method by JADE.

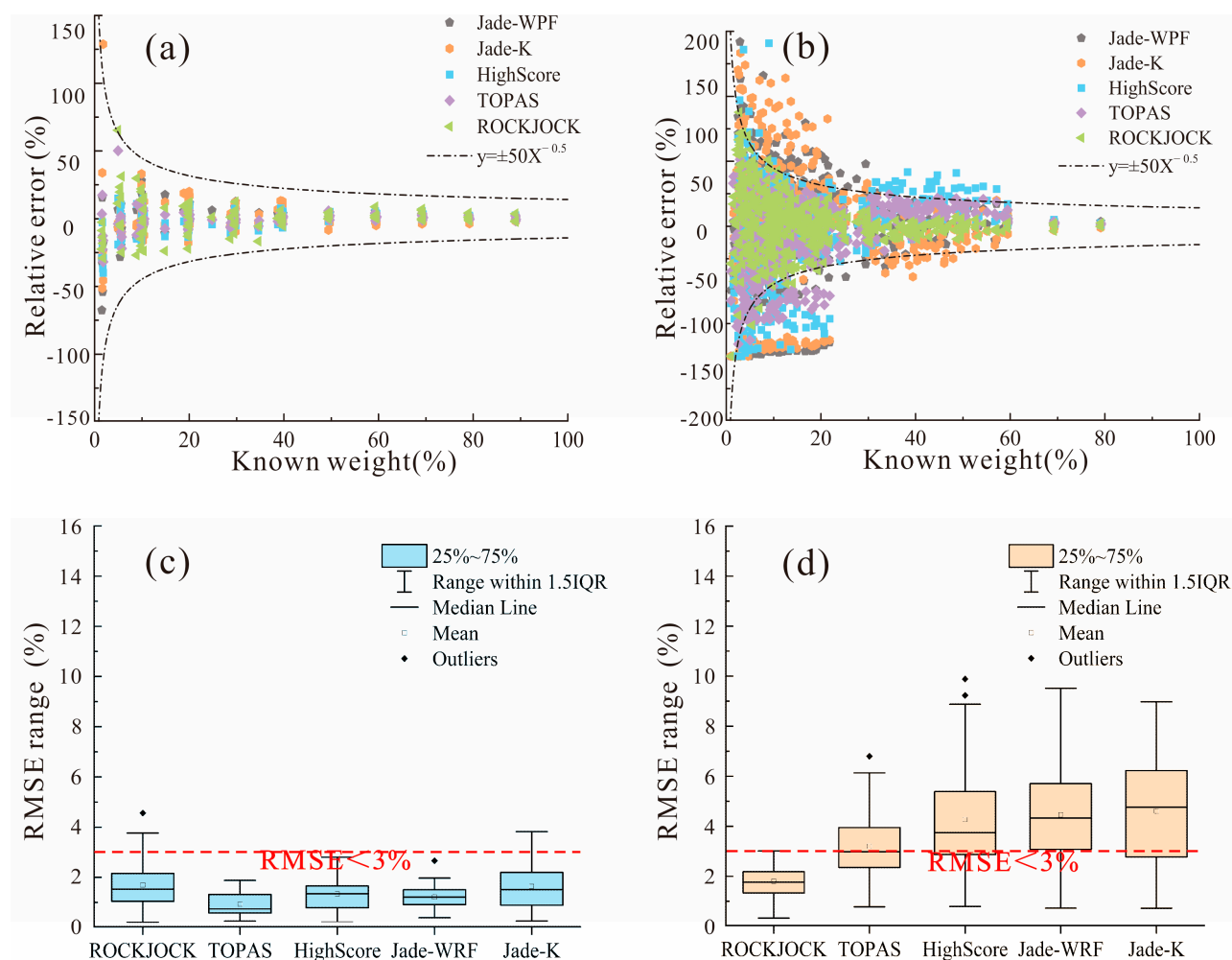


Figure 6. Scatter plot of the relative error (Δ_{RE}) of each phase and the root mean square error (RMSE) box pattern of each quantitative analysis method of sample. (a,c) are the mixture samples without clay minerals; (b,d) are the mixture samples containing clay minerals.

Overall, the results show that all kinds of quantitative methods have high accuracy for well-crystallized non-clay mixtures compared to clay-mineral-containing mixtures, which is demonstrated well by these mathematical statistical results (Figures 5 and 6c). In particular, the calculated RMSE results show that TOPAS has the greatest accuracy in quantifying samples without clay minerals (Figure 6c). In contrast, clay minerals are seriously underestimated by most quantitative methods for samples containing clay minerals such as montmorillonite, which results in the Δ_{AE} and the value of RMSE being significantly increased (Figures 5 and 6d). It is clear that the ROCKJOCK is the only one that can yield acceptable quantitative analysis results and has the lowest RMSE for multiphase systems containing clay minerals (Figure 6b,d). Therefore, we hypothesized that setting the threshold of RMSE within 3% would be a good way to evaluate the quantitative error of the crystalline phase system, which would be more appropriate than the Δ_{AE} within 3% applied in previous research.

4. Discussion

4.1. LOD

The LOD of each mineral phase is a cornerstone of the XRD measurement, which is employed to quantitatively evaluate a certain signal-to-noise rate [55]. It is related to the light intensity of the X-ray tube, test conditions, mass absorption coefficient, and crystallinity of the sample. Because the corundum used as the standard material has the

same crystallinity and mass absorption coefficient, the lower experimental results could be attributed to the internal properties of the instrument, such as the X-ray tube intensity and the radiation materials. This agrees with the findings that the LOD of Cu radiation is lower than that of Mo radiation [56].

The results show that the LOD is 0.10% for dolomite and 0.06% for calcite (Table 2), which are superior to the technique of Fourier transform infrared spectroscopy (FTIR) [57,58]. Even though the FTIR proves to be a useful complementary quantitative method for certain minerals such as kaolinite, carbonates, and some Fe oxides, the similarities in the spectra of the silicates (band coincidences) and the spectra band intensity affected by grain size make it unlikely to replace XRD for quantitative analysis [59–62]. These results highlight the advantage of the identification and quantification of minerals by XRD.

4.2. Accuracy

The influence of the LOD on the results can be safely ruled out by the fact that the artificially configured experimental concentration exceeds the LOD measured in our experiments. Therefore, we only compare and consider the specific performance and its miscellaneous causes between these quantitative methods in this study. Previous studies documented that the quantification of clay minerals remains complex due to their highly variable chemical compositions and structures [5,63–67], and our results also prove this. The asymmetric (100) peak of montmorillonite in Figure 1 shows that there is disordered stacking of unit cell in its crystalline structure, which is the main reason for the underestimation of its quantitative results in this experiment. In fact, the mixed-layered clay minerals such as weathering products are ubiquitous in exogenous geological environments, which usually develop disordered stacking structures and generate complex and variable diffraction patterns [68].

The ROCKJOCK yielded a relatively stable and accurate quantitative result (Figure 5a) because the FPS method obtains the relative weight of each phase by using their integrated intensities based on the Solver function in Microsoft Excel [21], with no need for the crystallographic data and RIR of each phase. These results corroborate that the asymmetric diffraction patterns caused by lattice distortion and disordered stacking would have a great impact on the Rietveld and RIR methods [67] but little on the FPS method. It may be explained by the fact that the integrated intensity of each phase is essentially constant in theory, which is not influenced by variable diffraction patterns. Thus, the FPS method can effectively eliminate the effect of the mineral crystallite variability [69].

The Rietveld method presents the highest accuracy of quantitative analysis for known crystallographic structures and non-clay minerals, especially the TOPAS software (version 6.0) (Figure 6c). It is well known that several common minerals always exhibit their preferred orientation resulting from cleavage or their layered crystal structure, such as feldspars, carbonates, and clay minerals [47,70]. The comparison of quantitative results of the non-clay samples showed that the Rietveld method appears to overcome the problem about the preferred orientation. On the other hand, the accuracy of Rietveld is greatly reduced for clay-mineral-containing samples (Figure 6d), partly due to the lack of a specific crystallographic structure model for clay minerals. More importantly, many clay minerals also show structural disorder effects, which change the intensity distribution of diffraction patterns and renders the usual Rietveld codes useless for structure refinement [71]. Despite great progress in modelling disordered stacking structures via the recursive calculation of structural factors [72–76], only a few details can be refined.

The JADE shows the largest Δ_{AE} value, which indicates that the RIR method produces a relatively low analytical accuracy for clay minerals. There are many reasons resulting in the reduction in accuracy of this single-peak quantitative method. Firstly, the RIR value, which determines the performance of this quantitative method, is often highly uncertain due to the polymorphism and isomorphism [47]. For example, the RIR value of montmorillonite varies considerably from 5.51 to 19.22, which could substantially underestimate

the proportion of montmorillonite. The occupancies and positions of interlayer water molecules and the layer spacing of the montmorillonite vary under the different prepared and measured conditions [73], which cause the instability of RIR values. Therefore, the choice of a standard RIR value is a crucial step. At the same time, there are many reference materials without RIR values in the database. On the other hand, as phyllosilicates, clay minerals present a strong tendency for a preferred orientation during sample preparation. In addition, nanocrystals of autogenic minerals are commonly contained in sediments, resulting in broadening of the diffraction peak and a significant deviation in quantitation using the RIR method [77]. It shows the obvious limitations of the RIR quantitative method in practice.

4.3. Applicability

The absolute errors of each quantification method are listed in Table 3. The comparison between these datasets shows that the accuracy obtained in this study is slightly less than those from the previous studies. Although the analysis accuracy will be improved by adding internal standards (e.g., corundum, zirconite), it can also lead to a tedious experimental and data process. Consequently, we still place an emphasis on the applicability of the XRD quantitative analysis without standards. In doing so, characteristics of the different methods used in this study are discussed in the following.

Table 3. A summary of analytical accuracies of various quantitative methods for phyllosilicate clay minerals.

Methods	Programs	Type of Samples	Number of Samples	Absolute Error Range (wt%)	References
Rietveld	MDI -Jade 6.0	artificial	5	−6.32%~+5.00%	(Zhao and Tan, 2018) [15]
	SIROQUANT	artificial	5	−5.9%~+10.9%	(Hillier, 2000) [47]
	HighScore	nature	/	±10%	(Kemp et al., 2016) [48]
	BGMN	artificial	4	±4.2%	(Ufer et al., 2012) [73] (Kleeberg et al., 2008) [70]
	HighScore/TOPAS	artificial	132	−12%~+10%	this study
FPS	ROCKJOCK	artificial	3	−7%~+3.1%	(Eberl, 2003) [21]
		artificial	3	−4.1%~+5.4%	
	ROCKJOCK	artificial	132	−7%~+6%	this study
RIR	/	artificial	5	−4.2%~+11.2%	(Hillier, 2000) [47]
	MDI -Jade 9.0	artificial	132	−19.2%~+17.4%	this study

Although the greatest advantage of the FPS method is its much higher analytical accuracy for clay minerals, its accuracy mostly relies on the pure materials library where diffraction patterns should be obtained under the same instrumental settings and experimental conditions [20]. Fortunately, the ROCKJOCK software can autocorrect the instrument and pure materials' parameters by input corundum diffraction data, making it more universal and convenient for practical analysis. Moreover, the FPS method is friendly to users with little knowledge of crystal structure [20] and suitable to both ordered and disordered materials, even amorphous materials. However, it is very computationally intensive and time-consuming for these circular iterative calculations. In spite of many programs being developed to improve the computational efficiency, they lack an accuracy evaluation system to ensure reliable results during quantitative analysis without standard materials.

The accuracy of the Rietveld method primarily depends on the quality of refinement [67], which is related to the adjustment of complex parameters, such as preferential orientation, test conditions, background, peak shape functions, and the correction of structural

parameters [78]. The Rietveld-based technique can correct these refinable parameters to improve the fitting effect, which reduces the impact caused by the overlapping reflections and preferred orientation. This sophisticated parametric refinement process has become highly automatic with the development and popularization of numerous software applications for the Rietveld method. However, despite the refinement procedure itself being automatic, the selection of structural models and refinable parameters, which have a strong influence on the results, is clearly dependent on users' experience and detailed crystallographic knowledge [71]. Furthermore, this method is calculated based on the assumption that the crystal structure of the sample is characterized by three-dimensional periodicity, which is valid for highly crystalline minerals, not for clay minerals. Consequently, not all Rietveld programs are capable of adequately modelling disordered phases or phases with unknown structures. However, it is worth noting that underestimating clay minerals mainly led to a significant deviation in quartz content, with relatively little effect on carbonate minerals and feldspar for TOPAS (version 6.0) and HighScore (version 3.0). Thus, this method of quantitative analysis can be desirable for samples containing clay minerals if only a specific type of mineral is quantified.

Our results show that the RIR method is the fastest quantitative approach. It is appropriate for powder samples including few well-crystallized mineral phases. However, this single-peak method is often plagued by preferred orientation and peak overlap issues, let alone the disordered minerals. Therefore, it should be applied carefully in complex samples [30]. Most importantly, the uncertainty or absence of RIR values would directly affect analysis accuracy. Thus, analysis accuracy is the biggest stumbling block in the application of the RIR method.

It is noted that the quality of quantification is deeply influenced by sample preparation, and measurement conditions are as important as the choice of analytical methods [30,71]. However, the latter is often ignored by researchers due to the lack of systematic understanding. Moreover, the accuracy of quantitative analysis is inevitably compromised in the face of hundreds and thousands of samples. As a result, many factors should be taken into account for the selection of these methods, such as the geological background, sampling environment, the number of samples, analysis time, etc. It is also necessary to supplement other analytical techniques for accuracy assessment and cross-validation to avoid erroneous conclusions regarding the validity of the analysis data [79–81], especially for samples containing clay minerals.

5. Conclusions

The determination of mineral composition and concentration is an important task for the investigation of paleoclimate and paleoenvironmental changes. XRD is currently a powerful quantitative analysis approach. This study evaluates the accuracy of the Rietveld, RIR, and FPS methods in the mineral quantitative analysis based on the ROCKJOCK, TOPAS (version 6.0), HighScore (version 3.0), and JADE software (version 9.0). The results show that these methods are substitutable for well-crystallized samples without a clay mineral phase owing to their generally consistent accuracy, while there are many different performances for clay samples during quantitative analysis. The advantage of the FPS method is its wide applicability. However, it is difficult to guarantee reliable quantitative results due to the absence of a results evaluation system if no additional standard materials are added. Although the problems of overlapping peaks and preferential orientation have been greatly improved by the Rietveld method, there are many limitations and difficulties for quantifying disordered phases using the method. The RIR technique is a simple and quick analytical method. Nevertheless, its accuracy relies heavily on the RIR value of the mineral. Therefore, the choice of these methods should be made on a case-by-case basis.

Supplementary Materials: The following supporting information can be downloaded at: <https://www.mdpi.com/article/10.3390/min13040566/s1>. Table S1: The comparison of weight and software analysis data for artificial mixture samples.

Author Contributions: Conceptualization, Y.S. and J.X.; writing—original draft preparation, J.X.; writing—review and editing, Y.S. and Y.L.; software, J.X.; methodology, J.X. and Y.S.; experiment, J.X.; supervision, Y.S. and Y.L.; project administration, Y.S.; funding acquisition, Y.S. All authors have read and agreed to the published version of the manuscript.

Funding: This research was funded by the Strategic Priority Research Program of Chinese Academy of Sciences (Grant no: XDB40000000), the Natural Science Foundation of China (Grant no: 41977385), and the State Key Laboratory of Loess and Quaternary Geology (Grant no: SKLLQGPY2006).

Data Availability Statement: Not applicable.

Acknowledgments: We express our heartfelt thanks to Stephen Hillier from the James Hutton Institute (UK) for his help through discussion, and Long Ma in Northwest University for their help with TOPAS.

Conflicts of Interest: The authors declare no conflict of interest.

Appendix A

R Core Team, 2019. R: A language and environment for statistical computing. Vienna, Austria: R Foundation for Statistical Computing. Retrieved from <https://www.R-project.org/> (accessed on 3 May 2022).

References

1. Bristow, T.F.; Rampe, E.B.; Achilles, C.N.; Blake, D.F.; Chipera, S.J.; Craig, P.; Crisp, J.A.; Des Marais, D.J.; Downs, R.T.; Gellert, R. Clay mineral diversity and abundance in sedimentary rocks of Gale crater, Mars. *Sci. Adv.* **2018**, *4*, eaar3330. [[CrossRef](#)]
2. Thorpe, M.T.; Hurowitz, J.A.; Dehouck, E. Sediment geochemistry and mineralogy from a glacial terrain river system in southwest Iceland. *Geochim. Cosmochim. Acta* **2019**, *263*, 140–166. [[CrossRef](#)]
3. Liu, Z.; Zhao, Y.; Colin, C.; Statterger, K.; Wiesner, M.G.; Huh, C.-A.; Zhang, Y.; Li, X.; Sompongchaiyakul, P.; You, C.-F. Source-to-sink transport processes of fluvial sediments in the South China Sea. *Earth Sci. Rev.* **2016**, *153*, 238–273. [[CrossRef](#)]
4. Tzvetanova, Y.; Petrov, O.; Kerestedjian, T.; Tarassov, M. Quantitative Phase Analysis of Skarn Rocks by the Rietveld Method Using X-ray Powder Diffraction Data. *Minerals* **2020**, *10*, 894. [[CrossRef](#)]
5. Ali, A.; Chiang, Y.W.; Santos, R.M. X-ray Diffraction Techniques for Mineral Characterization: A Review for Engineers of the Fundamentals, Applications, and Research Directions. *Minerals* **2022**, *12*, 205. [[CrossRef](#)]
6. Szopa, K.; Skreczko, S.; Chew, D.; Krzykowski, T.; Szymczyk, A. Multi-Tool (LA-ICPMS, EMPA and XRD) Investigation on Heavy Minerals from Selected Holocene Peat-Bog Deposits from the Upper Vistula River Valley, Poland. *Minerals* **2020**, *10*, 9. [[CrossRef](#)]
7. Andrade, G.R.P.; de Azevedo, A.C.; Lepchak, J.K.; Assis, T.C. Weathering of Permian sedimentary rocks and soil clay minerals transformations under subtropical climate, southern Brazil (Paraná State). *Geoderma* **2019**, *336*, 31–48. [[CrossRef](#)]
8. Fang, Q.; Hong, H.; Algeo, T.J.; Huang, X.; Sun, A.; Churchman, G.J.; Chorover, J.; Chen, S.; Liu, Y. Microtopography-mediated hydrologic environment controls elemental migration and mineral weathering in subalpine surface soils of subtropical monsoonal China. *Geoderma* **2019**, *344*, 82–98. [[CrossRef](#)]
9. Fang, Q.; Hong, H.; Furnes, H.; Chorover, J.; Luo, Q.; Zhao, L.; Algeo, T.J. Surficial weathering of kaolin regolith in a subtropical climate: Implications for supergene pedogenesis and bedrock argillization. *Geoderma* **2019**, *337*, 225–237. [[CrossRef](#)]
10. Hong, H.; Ji, K.; Hei, H.; Wang, C.; Liu, C.; Zhao, L.; Lanson, B.; Zhao, C.; Fang, Q.; Algeo, T.J. Clay mineral evolution and formation of intermediate phases during pedogenesis on picrite basalt bedrock under temperate conditions (Yunnan, southwestern China). *Catena* **2023**, *220*, 1–15. [[CrossRef](#)]
11. Fang, X.; Galy, A.; Yang, Y.; Zhang, W.; Ye, C.; Song, C. Paleogene global cooling-induced temperature feedback on chemical weathering, as recorded in the northern Tibetan Plateau. *Geology* **2019**, *47*, 992–996. [[CrossRef](#)]
12. Kemp, S.J.; Ellis, M.A.; Mountney, I.; Kender, S. Palaeoclimatic implications of high-resolution clay mineral assemblages preceding and across the onset of the Palaeocene-Eocene Thermal Maximum, North Sea Basin. *Clay Miner.* **2016**, *51*, 793–813. [[CrossRef](#)]
13. Hong, H.; Churchman, G.J.; Yin, K.; Li, R.; Li, Z. Randomly interstratified illite-vermiculite from weathering of illite in red earth sediments in Xuancheng, southeastern China. *Geoderma* **2014**, *214*, 42–49. [[CrossRef](#)]
14. Hong, H.; Churchman, G.J.; Gu, Y.; Yin, K.; Wang, C. Kaolinite-smectite mixed-layer clays in the Jiujiang red soils and their climate significance. *Geoderma* **2012**, *173*, 75–83. [[CrossRef](#)]
15. Zhao, W.; Tan, W.-F. Quantitative and structural analysis of minerals in soil clay fractions developed under different climate zones in China by XRD with Rietveld method, and its implications for pedogenesis. *Appl. Clay Sci.* **2018**, *162*, 351–361. [[CrossRef](#)]
16. Warr, L.N. Earth's clay mineral inventory and its climate interaction: A quantitative assessment. *Earth Sci. Rev.* **2022**, *234*, 1–37. [[CrossRef](#)]
17. Popovic, S.; Grzetaplenkovic, B.; Baliczunic, T. The Doping Method in Quantitative X-ray-Diffraction Phase-Analysis—Addendum. *J. Appl. Crystallogr.* **1983**, *16*, 505–507. [[CrossRef](#)]

18. Leroux, J.; Lennox, D.H.; Kay, K. Direct Quantitative X-ray Analysis by Diffraction-Absorption Technique. *Anal. Chem.* **1953**, *25*, 740–743. [[CrossRef](#)]
19. Smith, D.K.; Johnson, G.G.; Scheible, A.; Wims, A.M.; Johnson, J.L.; Ullmann, G. Quantitative X-ray powder diffraction method using the full diffraction pattern. *Powder Diffr.* **1987**, *2*, 73–77. [[CrossRef](#)]
20. Chipera, S.J.; Bish, D.L. FULLPAT: A full-pattern quantitative analysis program for X-ray powder diffraction using measured and calculated patterns. *J. Appl. Crystallogr.* **2002**, *35*, 744–749. [[CrossRef](#)]
21. Eberl, D.D. *User Guide to RockJock—A Program for Determining Quantitative Mineralogy from X-ray Diffraction Data*; US Geological Survey: Boulder, CO, USA, 2003. [[CrossRef](#)]
22. Butler, B.M.; Hillier, S. Automated Full-Pattern Summation of X-ray Powder Diffraction Data for High-Throughput Quantification of Clay-Bearing Mixtures. *Clays Clay Miner.* **2021**, *69*, 38–51. [[CrossRef](#)]
23. Chung, F.H. Quantitative Interpretation of X-ray-Diffraction Patterns of Mixtures. 2. Adiabatic Principle of X-ray-Diffraction Analysis of Mixtures. *J. Appl. Crystallogr.* **1974**, *7*, 526–531. [[CrossRef](#)]
24. Chung, F.H. Quantitative Interpretation of X-ray-Diffraction Patterns of Mixtures. 1. Matrix-Flushing Method for Quantitative Multicomponent Analysis. *J. Appl. Crystallogr.* **1974**, *7*, 519–525. [[CrossRef](#)]
25. Chung, F.H. Quantitative Interpretation of X-ray-Diffraction Patterns of Mixtures. 3. Simultaneous Determination of a Set of Reference Intensities. *J. Appl. Crystallogr.* **1975**, *8*, 17–19. [[CrossRef](#)]
26. Rietveld, H.M. Line Profiles of Neutron Powder-Diffraction Peaks for Structure Refinement. *Acta Crystallogr.* **1967**, *22*, 151. [[CrossRef](#)]
27. Rietveld, H.M. A Profile Refinement Method for Nuclear and Magnetic Structures. *J. Appl. Crystallogr.* **1969**, *2*, 65. [[CrossRef](#)]
28. Hillier, S. Quantitative analysis of clay minerals and poorly ordered phases by prior determined X-ray diffraction full pattern fitting: Procedures and prospects. In Proceedings of the 9th Mid-European Clay Conference, Zagreb, Croatia, 17–21 September 2018; p. 6.
29. Zhou, X.; Liu, D.; Bu, H.; Deng, L.; Liu, H.; Yuan, P.; Du, P.; Song, H. XRD-based quantitative analysis of clay minerals using reference intensity ratios, mineral intensity factors, Rietveld, and full pattern summation methods: A critical review. *Solid Earth Sci.* **2018**, *3*, 16–29. [[CrossRef](#)]
30. Omotoso, O.; McCarty, D.K.; Hillier, S.; Kleeberg, R. Some successful approaches to quantitative mineral analysis as revealed by the 3rd Reynolds Cup contest. *Clays Clay Miner.* **2006**, *54*, 748–760. [[CrossRef](#)]
31. Raven, M.D.; Self, P.G. Outcomes of 12 years of the Reynolds Cup quantitative mineral analysis round robin. *Clays Clay Miner.* **2017**, *65*, 122–134. [[CrossRef](#)]
32. Chipera, S.J.; Bish, D.L. Fitting full X-ray diffraction patterns for quantitative analysis: A method for readily quantifying crystalline and disordered phases. *Adv. Mater. Phys. Chem.* **2013**, *3*, 47–53. [[CrossRef](#)]
33. Bish, D.L.; Howard, S.A. Quantitative Phase-Analysis Using the Rietveld Method. *J. Appl. Crystallogr.* **1988**, *21*, 86–91. [[CrossRef](#)]
34. Bish, D.L.; Post, J.E. Quantitative Mineralogical Analysis Using the Rietveld Full-Pattern Fitting Method. *Am. Mineral.* **1993**, *78*, 932–940.
35. Hillier, S. Quantitative analysis of clay and other minerals in sandstones by X-ray powder diffraction (XRPD). In *Clay Mineral Cements in Sandstones*; Worden, R., Morad, S., Eds.; Blackwell Publishing: Oxford, UK, 1999; pp. 213–251. ISBN 9781444304336.
36. Westphal, T.; Füllmann, T.; Pöllmann, H. Rietveld quantification of amorphous portions with an internal standard—Mathematical consequences of the experimental approach. *Powder Diffr.* **2009**, *24*, 239–243. [[CrossRef](#)]
37. Zhao, P.Q.; Lu, L.C.; Liu, X.P.; De la Torre, A.G.; Cheng, X. Error Analysis and Correction for Quantitative Phase Analysis Based on Rietveld-Internal Standard Method: Whether the Minor Phases Can Be Ignored? *Crystals* **2018**, *8*, 110. [[CrossRef](#)]
38. Degen, T.; Sadki, M.; Bron, E.; Konig, U.; Nenert, G. The HighScore suite. *Powder Diffr.* **2014**, *29*, S13–S18. [[CrossRef](#)]
39. Coelho, A.A. TOPAS and TOPAS-Academic: An optimization program integrating computer algebra and crystallographic objects written in C++. *J. Appl. Crystallogr.* **2018**, *51*, 210–218. [[CrossRef](#)]
40. Toby, B.H. EXPGUI, a graphical user interface for GSAS. *J. Appl. Crystallogr.* **2001**, *34*, 210–213. [[CrossRef](#)]
41. Doebelin, N.; Kleeberg, R. Profex: A graphical user interface for the Rietveld refinement program BGMN. *J. Appl. Crystallogr.* **2015**, *48*, 1573–1580. [[CrossRef](#)]
42. Taut, T.; Kleeberg, R.; Bergmann, J. Seifert Software: The new Seifert Rietveld program BGMN and its application to quantitative phase analysis. *Mater. Struct.* **1998**, *5*, 57–66.
43. Lutterotti, L. Maud: A Rietveld analysis program designed for the internet and experiment integration. *Acta Crystallogr. A* **2000**, *56*, s54. [[CrossRef](#)]
44. Madse, I.; Hill, R. Rietveld analysis using para> focusing and Debye-Scherrer geometry data collected with a Bragg-Brentano diffractometer. *Z. Krist. Cryst. Mater.* **1991**, *196*, 73–92. [[CrossRef](#)]
45. Young, R.; Prince, E.; Sparks, R. Suggested guidelines for the publication of Rietveld analyses and pattern decomposition studies. *J. Appl. Crystallogr.* **1982**, *15*, 357–359. [[CrossRef](#)]
46. Young, R.A. *The Rietveld Method*; Oxford University Press: New York, NY, USA, 1993; ISBN 0198555776.
47. Hillier, S. Accurate quantitative analysis of clay and other minerals in sandstones by XRD: Comparison of a Rietveld and a reference intensity ratio (RIR) method and the importance of sample preparation. *Clay Miner.* **2000**, *35*, 291–302. [[CrossRef](#)]
48. Kemp, S.; Smith, F.; Wagner, D.; Mounteney, I.; Bell, C.; Milne, C.; Gowing, C.; Pottas, T. An improved approach to characterize potash-bearing evaporite deposits, evidenced in North Yorkshire, United Kingdom. *Econ. Geol.* **2016**, *111*, 719–742. [[CrossRef](#)]

49. Hughes, H.; Hurley, P.W. Precision and Accuracy of Test Methods and the Concept of K-Factors in Chemical-Analysis. *Analyst* **1987**, *112*, 1445–1449. [[CrossRef](#)]
50. Calvert, C.; Palkowsky, D.; Pevear, D. A combined X-ray powder diffraction and chemical method for the quantitative mineral analysis of geologic samples. In *Quantitative Mineral Analysis of Clays*; Clay Minerals Society: Austin, TX, USA, 1989; ISBN 9781881208211.
51. Paz, S.; Torres, P.; Angélica, R.; Kahn, H. Synthesis, Rietveld refinement and DSC analysis of Al-goethites to support mineralogical quantification of gibbsitic bauxites. *J. Therm. Anal. Calorim.* **2017**, *128*, 841–854. [[CrossRef](#)]
52. Prandel, L.V.; Dias, N.M.P.; da Costa Saab, S.; Brinatti, A.M.; Giarola, N.F.B.; Pires, L.F. Characterization of kaolinite in the hardsetting clay fraction using atomic force microscopy, X-ray diffraction, and the Rietveld method. *J. Soils Sediments* **2017**, *17*, 2144–2155. [[CrossRef](#)]
53. Uvarov, V. The influence of X-ray diffraction pattern angular range on Rietveld refinement results used for quantitative analysis, crystallite size calculation and unit-cell parameter refinement. *J. Appl. Crystallogr.* **2019**, *52*, 252–261. [[CrossRef](#)]
54. Toby, B.H. R factors in Rietveld analysis: How good is good enough? *Powder Diffr.* **2006**, *21*, 67–70. [[CrossRef](#)]
55. Davis, B.L. The estimation of limits of detection in RIM quantitative X-ray diffraction analysis. *Advances in X-ray. Analysis* **1987**, *31*, 317–323. [[CrossRef](#)]
56. Leon-Reina, L.; Garcia-Mate, M.; Alvarez-Pinazo, G.; Santacruz, I.; Vallcorba, O.; de la Torre, A.G.; Aranda, M.A.G. Accuracy in Rietveld quantitative phase analysis: A comparative study of strictly monochromatic Mo and Cu radiations. *J. Appl. Crystallogr.* **2016**, *49*, 722–735. [[CrossRef](#)] [[PubMed](#)]
57. Meng, X.; Liu, L.; Wang, X.T.; Balsam, W.; Chen, J.; Ji, J. Mineralogical evidence of reduced East Asian summer monsoon rainfall on the Chinese loess plateau during the early Pleistocene interglacials. *Earth Planet Sci. Lett.* **2018**, *486*, 61–69. [[CrossRef](#)]
58. Vyverberg, K.L.; Jaeger, J.M.; Dutton, A. Quantifying detection limits and uncertainty in X-ray diffraction mineralogical assessments of biogenic carbonates. *J. Sediment. Res.* **2018**, *88*, 1261–1275. [[CrossRef](#)]
59. Mansfeldt, T.; Schuth, S.; Häusler, W.; Wagner, F.E.; Kaufhold, S.; Overesch, M. Iron oxide mineralogy and stable iron isotope composition in a Gleysol with petrogleyic properties. *J. Soils Sediments* **2012**, *12*, 97–114. [[CrossRef](#)]
60. Craddock, P.R.; Herron, M.M.; Herron, S.L. Comparison of quantitative mineral analysis by X-ray diffraction and Fourier transform infrared spectroscopy. *J. Sediment. Res.* **2017**, *87*, 630–652. [[CrossRef](#)]
61. Hassaan, M.A.; El Nemr, A. Classification and identification of different minerals in the Mediterranean sediments using PSA, FTIR, and XRD techniques. *Mar. Pollut. Bull.* **2021**, *173*, 113070. [[CrossRef](#)]
62. Kaufhold, S.; Hein, M.; Dohrmann, R.; Ufer, K. Quantification of the mineralogical composition of clays using FTIR spectroscopy. *Vib. Spectrosc.* **2012**, *59*, 29–39. [[CrossRef](#)]
63. Środoń, J.; Drits, V.A.; McCarty, D.K.; Hsieh, J.C.C.; Eberl, D.D. Quantitative X-ray diffraction analysis of clay-bearing rocks from random preparations. *Clays Clay Miner.* **2001**, *49*, 514–528. [[CrossRef](#)]
64. Środoń, J. Quantitative mineralogy of sedimentary rocks with emphasis on clays and with applications to K-Ar dating. *Miner. Mag.* **2002**, *66*, 677–687. [[CrossRef](#)]
65. Cuevas, J.; Cabrera, M.A.; Fernandez, C.; Mota-Heredia, C.; Fernandez, R.; Torres, E.; Turrero, M.J.; Ruiz, A.I. Bentonite Powder XRD Quantitative Analysis Using Rietveld Refinement: Revisiting and Updating Bulk Semiquantitative Mineralogical Compositions. *Minerals* **2022**, *12*, 772. [[CrossRef](#)]
66. Bish, D.L.; Reynolds, R. *Advanced Computational Analysis of Disordered Materials and Clay Minerals*; Los Alamos National Lab. (LANL): Los Alamos, NM, USA, 2001.
67. Środoń, J. Identification and quantitative analysis of clay minerals. *Dev. Clay Sci.* **2013**, *5*, 25–49. [[CrossRef](#)]
68. Środoń, J. Nature of mixed-layer clays and mechanisms of their formation and alteration. *Annu. Rev. Earth Planet. Sci.* **1999**, *27*, 19–53. [[CrossRef](#)]
69. Moore, D.M.; Reynolds, R.C., Jr. *X-ray Diffraction and the Identification and Analysis of Clay Minerals*; Oxford University Press: New York, NY, USA, 1989; ISBN 0195087135.
70. Kleeberg, R.; Monecke, T.; Hillier, S. Preferred orientation of mineral grains in sample mounts for quantitative XRD measurements: How random are powder samples? *Clays Clay Miner.* **2008**, *56*, 404–415. [[CrossRef](#)]
71. Ufer, K.; Raven, M.D. Application of the Rietveld method in the Reynolds cup contest. *Clays Clay Miner.* **2017**, *65*, 286–297. [[CrossRef](#)]
72. Ufer, K.; Kleeberg, R.; Bergmann, J.; Dohrmann, R. Rietveld refinement of disordered illite-smectite mixed-layer structures by a recursive algorithm. I: One-dimensional patterns. *Clays Clay Miner.* **2012**, *60*, 507–534. [[CrossRef](#)]
73. Ufer, K.; Kleeberg, R.; Bergmann, J.; Dohrmann, R. Rietveld refinement of disordered illite-smectite mixed-layer structures by a recursive algorithm. II: Powder-pattern refinement and quantitative phase analysis. *Clays Clay Miner.* **2012**, *60*, 535–552. [[CrossRef](#)]
74. Ufer, K.; Roth, G.; Kleeberg, R.; Stanjek, H.; Dohrmann, R.; Bergmann, J. Description of X-ray powder pattern of turbostratically disordered layer structures with a Rietveld compatible approach. *Z. Kristallogr.* **2004**, *219*, 519–527. [[CrossRef](#)]
75. Ufer, K.; Kleeberg, R.; Bergmann, J.; Curtius, H.; Dohrmann, R. Refining real structure parameters of disordered layer structures within the Rietveld method. *Z. Kristallogr.* **2008**, *27*, 151–158. [[CrossRef](#)]

76. Dietel, J.; Ufer, K.; Kaufhold, S.; Dohrmann, R. Crystal structure model development for soil clay minerals—II. Quantification and characterization of hydroxy-interlayered smectite (HIS) using the Rietveld refinement technique. *Geoderma* **2019**, *347*, 1–12. [[CrossRef](#)]
77. Huang, Q.; Wang, C.; Shan, Q. Quantitative Deviation of Nanocrystals Using the RIR Method in X-ray Diffraction (XRD). *Nanomaterials* **2022**, *12*, 2320. [[CrossRef](#)]
78. Will, G. The Rietveld Method and the Two Stage Method to Determine and Refine Crystal Structures from Powder Diffraction Data. In *Powder Diffraction*; Springer Berlin: Heidelberg, Germany, 2006; ISBN 9783540279860.
79. Rahfeld, A.; Kleeberg, R.; Möckel, R.; Gutzmer, J. Quantitative mineralogical analysis of European Kupferschiefer ore. *Miner. Eng.* **2018**, *115*, 21–32. [[CrossRef](#)]
80. Cesarano, M.; Bish, D.; Cappelletti, P.; Cavalcante, F.; Belviso, C.; Fiore, S. Quantitative mineralogy of clay-rich siliciclastic landslide terrain of the Sorrento Peninsula, Italy, using a combined XRPD and XRF approach. *Clays Clay Miner.* **2018**, *66*, 353–369. [[CrossRef](#)]
81. Herron, S.; Herron, M.; Pirie, I.; Saldungaray, P.; Craddock, P.; Charsky, A.; Polyakov, M.; Shray, F.; Li, T. Application and quality control of core data for the development and validation of elemental spectroscopy log interpretation. *Petrophysics SPWLA J. Form. Eval. Reserv. Descr.* **2014**, *55*, 392–414.

Disclaimer/Publisher’s Note: The statements, opinions and data contained in all publications are solely those of the individual author(s) and contributor(s) and not of MDPI and/or the editor(s). MDPI and/or the editor(s) disclaim responsibility for any injury to people or property resulting from any ideas, methods, instructions or products referred to in the content.